Original Article

Comparative study of normal condyle and temporomandibular joint prosthesis movement during mouth opening by dynamic magnetic resonance imaging and computed tomography

Jun Wang[1#], Jiangshan Hua[2,3,4,5#], Ruoyi Ding[2,3,4,5#], Luxiang Zou[2,3,4,5], Haoyu Li[2,3,4,5], Luzhu Zhang[2,3,4,5], Qi Sun[6], Dongmei He[2,3,4,5]

[1]School of Mechanical Engineering, Tribology Research Institute, Southwest Jiao Tong University, Chengdu, China; [2]Department of Oral Surgery, Shanghai Ninth People's Hospital, Shanghai Jiao Tong University School of Medicine, Shanghai, China; [3]College of Stomatology, Shanghai Jiao Tong University, National Center for Stomatology, Shanghai, China; [4]National Clinical Research Center for Oral Diseases, Shanghai, China; [5]Shanghai Key Laboratory of Stomatology, Shanghai Research Institute of Stomatology, Shanghai, China; [6]Department of Radiology, Shanghai Ninth People's Hospital, Shanghai Jiao Tong University School of Medicine, Shanghai, China

Contributions: (I) Conception and design: D He; (II) Administrative support: D He; (III) Provision of study materials or patients: L Zhang, Q Sun; (IV) Collection and assembly of data: L Zhang, L Zou, H Li; (V) Data analysis and interpretation: J Wang, J Hua, R Ding; (VI) Manuscript writing: All authors; (VII) Final approval of manuscript: All authors.

[#]These authors contributed equally to this work and should be considered as co-first authors.

Correspondence to: Luzhu Zhang, DDS, MS. Department of Oral Surgery, Shanghai Ninth People's Hospital, Shanghai Jiao Tong University School of Medicine, Shanghai, China; College of Stomatology, Shanghai Jiao Tong University, National Center for Stomatology, Shanghai, China; National Clinical Research Center for Oral Diseases, Shanghai, China; Shanghai Key Laboratory of Stomatology, Shanghai Research Institute of Stomatology, Shanghai, China. Email: zhang.lu.zhu@qq.com; Qi Sun, ST. Department of Radiology, Shanghai Ninth People's Hospital, Shanghai Jiao Tong University School of Medicine, Shanghai, China. Email: xiaosi-qiqi@yeah.net; Dongmei He, DDS, MD. Department of Oral Surgery, Shanghai Ninth People's Hospital, Shanghai Jiao Tong University School of Medicine, Shanghai, China; College of Stomatology, Shanghai Jiao Tong University; National Center for Stomatology, Shanghai, China; National Clinical Research Center for Oral Diseases, Shanghai, China; Shanghai Key Laboratory of Stomatology, Shanghai Research Institute of Stomatology, Shanghai, China. Email: lucyhe119@163.com.

Background: To analyze and compare the trajectory of condylar motion during mouth opening in normal volunteers and patients after total joint replacement (TJR) of the temporomandibular joint (TMJ).

Methods: Condylar movement during mouth opening was recorded by dynamic magnetic resonance imaging (MRI) for volunteers with normal TMJs and dynamic computed tomography (CT) for patients after TMJ TJR. Trajectories of the points selected every 5 mm from the superior point of the condyle (P_0) along its axis to the mandibular angle (P_{-25}) were recorded. The arc length and curvature radius of average trajectories for each point were calculated and compared between the normal joints and TJRs, especially P_{-10} which is the corresponding point of the prosthesis apex without lateral pterygoid muscle (LPM) attachment at the normal joint with LPM attachment. The location of the point with the most similar trajectory was identified in the normal joints and compared with the condylar prosthesis.

Results: A total of 9 volunteers with 18 normal TMJs, and 5 patients with 6 prostheses were included in this study. For normal TMJs, the average condylar trajectories during mouth opening were a concave upward curve. Meanwhile, the trajectories of contralateral normal joints in patients with unilateral TJR and all condylar prostheses were significantly decreased. The arc length and curvature radius of average trajectories gradually decreased from P_0. In the normal joints, P_{-20} had the most similar trajectories with the average arc lengths and a curvature radius of 13.0/4.2 mm. In P_{-10}, the average arc lengths and curvature radius of the normal cases, natural TMJ of the unilateral replacement patients, prosthetic TMJ of the unilateral replacement patients, and prosthetic TMJ of the bilateral replacement patient, were 15.6/6.6 mm,

13.1/4.9 mm, 4.7/4.4 mm, and 6.4/5.8 mm, respectively.

Conclusions: P_{-20} in the normal joint exhibited the most similar trajectory among individuals. The trajectory difference between the prosthesis apex without LPM attachment and the corresponding point at the normal joint with LPM attachment provides a reference for fossa prosthesis functional surface design.

Keywords: Temporomandibular joint (TMJ); artificial total joint replacement; mandibular movement; dynamic magnetic resonance imaging; computed tomography (CT)

Submitted Nov 08, 2022. Accepted for publication Apr 11, 2023. Published online May 15, 2023.
doi: 10.21037/qims-22-1239
View this article at: https://dx.doi.org/10.21037/qims-22-1239

Introduction

Temporomandibular joint (TMJ) alloplastic total joint replacement (TJR) is widely accepted as a safe, effective, and reliable end-stage procedure for patients with severe TMJ conditions, such as advanced degenerative joint disease, tumors, developmental anomalies, and ankylosis (1). The main advantages of TJR are reduced intraoperative time, increased suitability, no risk of resorption, no need for a donor site, and bone grafts (2,3). TMJ Concepts (Stryker; Ventura, CA, USA) and Biomet/Lorenz (Jacksonville, FL, USA) are the most widely used alloplastic TMJ replacement systems. Long-term clinical studies have shown that both systems are effective in increasing maximum mouth opening and quality of life (4,5). However, many researchers have observed restrictions in protrusion and laterotrusion (5-7). The sliding distance of a condylar prosthesis is about 2 mm (7), which is much smaller than the 16 mm of a normal condyle (8). Previous studies have highlighted 2 main causes for the restriction: the loss of external (lateral) pterygoid muscle attachment and the formation of scar tissue around the surgical area (5,9,10). Additionally, the design of the glenoid fossa prosthesis also restricts the motion of the condylar prosthesis (7).

To restore mandibular movement after alloplastic TJR, the design of the prosthesis may need to be modified. This first requires quantifying the postoperative movement of the TMJ and mandible, as well as the kinematical difference between normal individuals and those who undergo TMJ TJR, especially the corresponding points on the normal condyle to the artificial condylar head, which has no lateral pterygoid muscle (LPM) attachment. This has not yet been described in the literature. There are numerous methods to measure mandibular kinematics (11-16), such as mandibular motion trajectory machines, which require auxiliary devices attached to the patient's face and teeth, and computed tomography (CT) scanning. However, these methods have common limitations. Firstly, it is difficult to quantify the impact of placing markers and/or measurement devices on the teeth and skin on kinematics when using these methods. Secondly, placing markers or devices on the skin will not make their movement completely consistent with that of the bone because of interference by skin, fat, and muscle between the markers or devices and bone. Although placing markers or devices on the teeth is an alternative method, it is not suitable for individuals with missing or unstable teeth.

Dynamic magnetic resonance imaging (MRI) and CT can record the mandibular movement directly without the need for auxiliary devices. Therefore, in this study, we used dynamic MRI (17-20) on volunteers with normal TMJ because, unlike CT, MRI has no radiation. Dynamic CT was employed for patients after TJR because the prosthesis cannot be seen clearly on MRI but is visible on CT. In our previous study, we designed a novel TMJ prosthesis for LPM attachment (21). By comparing the kinematics difference during mouth opening between normal TMJ and condylar prosthesis, we will modify the fossa prosthesis design to achieve improved mandibular prosthesis movement, which will provide a reference for a change in prosthesis design.

Methods

The study was conducted in accordance with the Declaration of Helsinki (as revised in 2013) and was approved by the Independent Ethics Committee of Shanghai Jiao Tong University School of Medicine Affiliated 9th People's Hospital (No. SH9H-2021-T111-2). Informed consent was provided by all individual participants.

The inclusion criteria for volunteers receiving dynamic MRI examination were as follows: (I) age ≥18 years; (II)

MRI showing normal disc and condyle relationship; (III) no history of TMJ disease or surgery; (IV) no maxillofacial deformity; and (V) normal occlusion and intact dentition.

The inclusion criteria for participants receiving dynamic CT were as follows: (I) accepted Biomet standard alloplastic TJR; (II) postoperative follow-up time of at least 6 months; (III) maximum incisor opening (MIO) ≥30 mm; and (IV) no pain, swelling, or discomfort in the TMJ area.

Dynamic MRI for normal TMJ

The scanning was performed using a 1.5 Tesla-Speed Excite system (GE Healthcare, Milwaukee, WI, USA) on the oblique sagittal position of the condyle. The fast imaging employing steady-state acquisition (FIESTA) MRI parameters were as follows: repetition time (TR): 3.6 ms; echo time (TE): 1.8 ms; slice thickness (SL)/SPACE: 5 mm/1 mm; field of view (FOV): 18 cm × 18 cm; MATRIX: 256×256; flip angle: 60°; number of excitations (NEX): 90 s; bandwidth: 125 kHz. All volunteers were instructed to perform an open-close mouth movement slowly. A total of 60 continuous images were obtained in 90 seconds. The images obtained were saved on a computer for further analysis (20).

Data analysis

A complete mouth-opening process was selected from the 60 continuous images obtained. The shapes of the condyle, ramus, and glenoid fossa in the selected images were traced. Next, the direction of the axis of the condylar head was determined using the 2 steps method described by Hu *et al.* (22): the first circle (O_1) was drawn tangentially to the anterior, posterior, and superior surfaces of the condylar head. The second circle (O_2) was drawn at the most curved area between the condylar head and neck. The center of the two circles determined the direction of the condylar axis (*Figure 1A*).

Then, the coordinate system was established as follows: (I) the vertex of the joint socket was set as the origin of the coordinate system; (II) the Y axis was set as the line passing through the origin and parallel to the condylar axis; (III) the X axis was set as the line passing through the origin and perpendicular to the Y axis. The intersection between the condylar axis and the superior surface of the condylar head determined the position of the top of the condyle (the first point, P_0). The following 5 points (P_{-5}, P_{-10}, P_{-15}, P_{-20}, P_{-25}) were set as the points 5 mm, 10 mm, 15 mm, 20 mm, and 25 mm down the first point (*Figure 1B*). The coordinates of P_0 to P_{-25} in each image was recorded (*Figure 1B-1H*). The line joining P_0 in each image in chronological order could preliminarily simulate the trajectory of P_0 (*Figure 2A*). Generating a smooth curve by discrete data to simulate the actual situation was performed by cubic splint data, mathematical method (23,24). The trajectories were smoothed using the splint function in MATLAB software (MathWorks, Natick, MA, US) (*Figure 2B*). The coordinates of 46 points were selected at equal intervals on the smoothed trajectory for subsequent analysis (*Figure 2C*).

There were 18 healthy TMJs included in the study, so 18 trajectories were obtained for P_0. The starting coordinate and shape of the trajectories can both affect the calculation of an average trajectory. To exclude the effect of the starting coordinate, 18 trajectories of P_0 were moved to the same starting coordinate. The average trajectory was determined by the location of 46 points and each point was an average of the coordinates of the corresponding points on the 18 trajectories (*Figure 3*). The average trajectories of P_{-5}, P_{-10}, P_{-15}, P_{-20}, and P_{-25} were calculated using the same procedure. The average trajectory shape was quantified by arc lengths and the average curvature radius. Arc length was approximately the sum of the length of the line segments between 46 points calculated by MATLAB software. The average curvature was determined by the curvature at 46 points calculated by ProE software (Parametric Technology Corporation, Boston, MA, USA).

The similarity of the 18 trajectories of P_0 was calculated by the Fréchet distance, which is a description of the similarity of the 2 trajectories proposed by the French mathematician Maurice René Fréchet (24). It can be colloquially defined as follows: a man is walking a dog on a leash and they move along 2 different curves. The Fréchet distance of these two curves is the shortest leash that allows the man and dog to travel through their paths (24). The Fréchet distance was calculated for each trajectory relative to the average trajectory. The sum of 18 Fréchet distances represented the similarity of the 18 trajectories of P_0. The other 11 points were calculated in the same way. A shorter Fréchet distance denoted better similarity of the trajectories. The point with the best similarity of trajectories was located and the arc length and average curvature radius

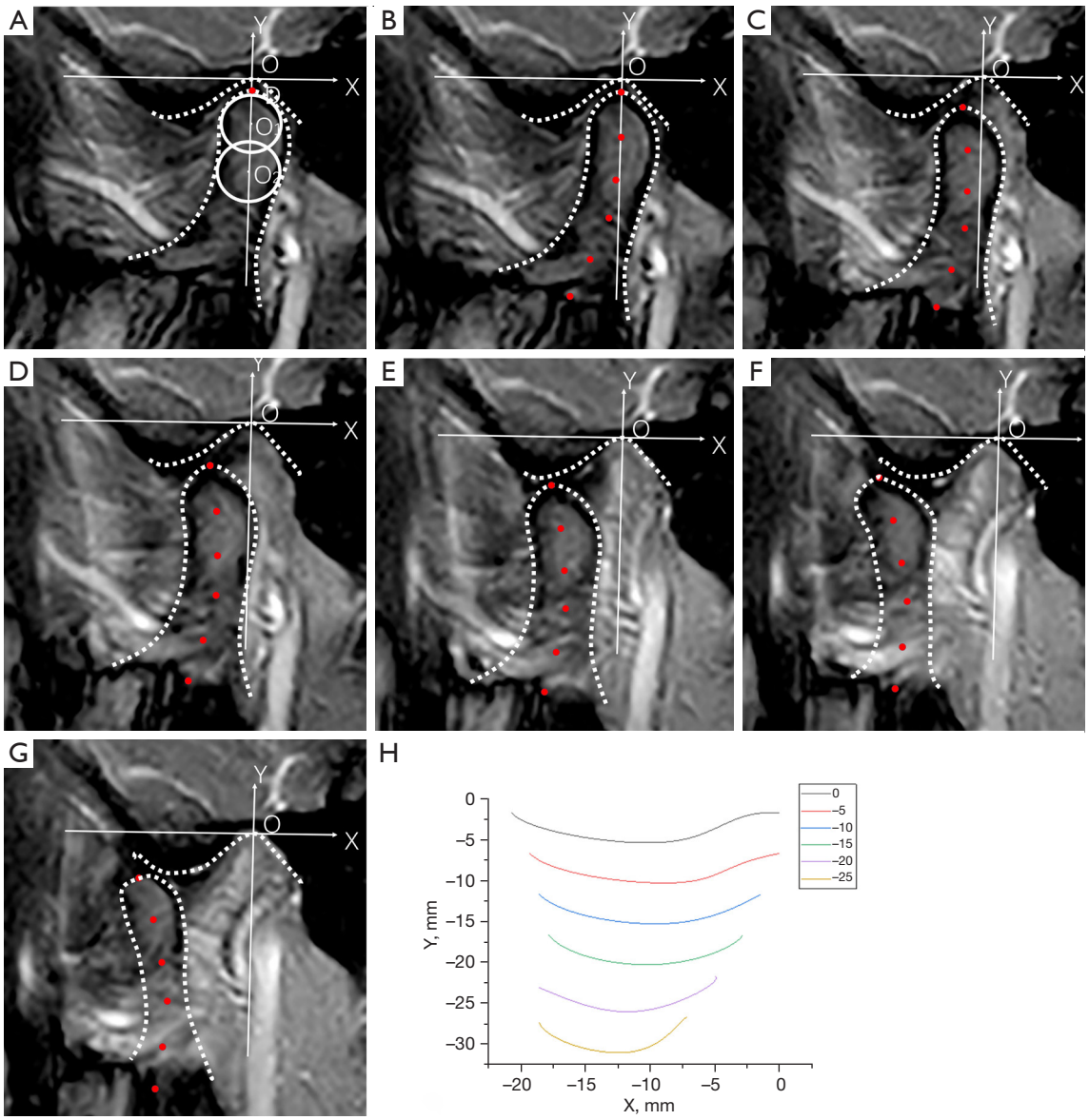

Figure 1 The procedure of obtaining the coordinate of 12 points of a volunteer. (A) The direction of the axis of condylar head was determined using the two steps method and the coordinate system was established. (B-G) The position of P_0 to P_{-55} were determined during mouth opening process. (H) Twelve trajectories were drawn and smoothed using MATLAB software (MathWorks, US).

of its average trajectory were clarified.

Dynamic CT for TMJ prosthesis

Dynamic CT scanning was performed using a 64-slice spiral Discovery CT (HD 750 CT; General Electric Company, Boston, MA, USA). The patient lay facing upwards so that the orbital ear plane was perpendicular to the horizontal plane. Each participant slowly opened their mouth from the intercuspal position to the maximum opening three times. The CT parameters were as follows: Patients' images were randomly captured at equal time intervals from the top of the skull to the lowest edge of the mandible, with a layer thickness of 0.625 mm. The scanning voltage was 120 kV and the bulb current was 284 mA. Digital imaging and communications in medicine (DICOM) data were imported into Proplan 1.4 (Materialise, Leuven, Belgium). By segmentation and reconstruction, 3-dimensional (3D)

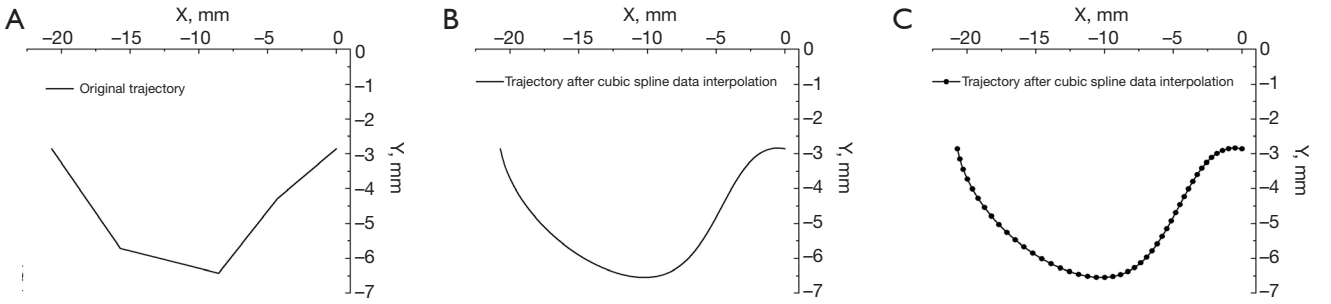

Figure 2 The preliminary simulation of a trajectory of P_0 and its further mathematical progressing. (A) The line joining P_0 in each image in chronological order could preliminarily simulate the trajectory of P_0; (B) the trajectory was smoothed using the splint function in MATLAB software; (C) the coordinate of 46 points were selected at equal interval on the smoothed trajectory for further analysis.

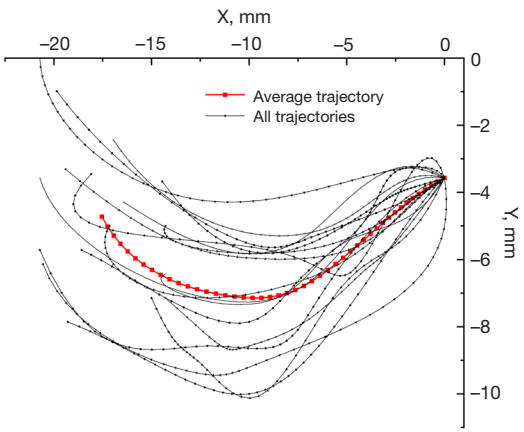

Figure 3 Calculation of the average trajectory of P_0. Eighteen trajectories of P_0 were moved to the same starting coordinate. Average trajectory was determined by the location of 46 points (red dots) and the coordinate of each point was an average of the corresponding points on the 18 trajectories (black dots).

images of the patient's skull in each frame were obtained and saved as standard triangle language (STL) files.

Data analysis

The above STL files were imported into the auto Geomagic Wrap 2015, and the maxilla and mandible were spatially fit at each frame according to the anatomical marker points of the maxilla to obtain the movement position of the jaw at each frame based on the maxilla. The reconstructed CT plain scan images at each time were cumulatively matched with the maxilla as the reference position to obtain the spatial position and range of continuous movement of the patient's condyle after artificial joint replacement (*Figure 4A*).

The triangular patch model (.STL) of the mandible was then converted into the point cloud model (.PCD). Taking the mandibule at the intercuspal position as the source point cloud and the others as the target point cloud, coarse registration and accurate registration were carried out successively. The initial registration was carried out by the 3D shape context (3DSC) method based on local features. The search radius of 3DSC registration was set to 0.5 mm. Accurate registration was performed using the iterative closest point (ICP). The iterations of ICP registration were set to 100. The maximum distance between the corresponding points was 0.01 mm. The threshold value of the difference between two adjacent iterations was set to 1e-10 [transformation epsilon, singular value decomposition (SVD)], and the threshold value of the sum of root mean square error (Euclidean fitness epsilon) was set to 0.01. The point cloud was randomly down-sampled to obtain a point cloud of 4,000 points based on Vitter (25) for calculation efficiency (*Figure 4B*). The final output result of point cloud registration was the rotation matrix R_i and translation vector t_i of the rigid transformation of the mandible from the intercuspal position frame to the i frame.

Spatial coordinates of the apex of bilateral condyles and the midpoint of maxillary and mandibular central incisors at the intercuspal position were determined in Geomagic Wrap 2015 (3D Systems, Rock Hill, SC, USA), and the spatial coordinate positions of these points in another frame were calculated using the formula below:

$$\alpha_i = R_i\alpha_1 + t_i \quad [1]$$

Where α_1 is the spatial coordinate position of a point at the intercuspal position frame, α_i is the spatial coordinate

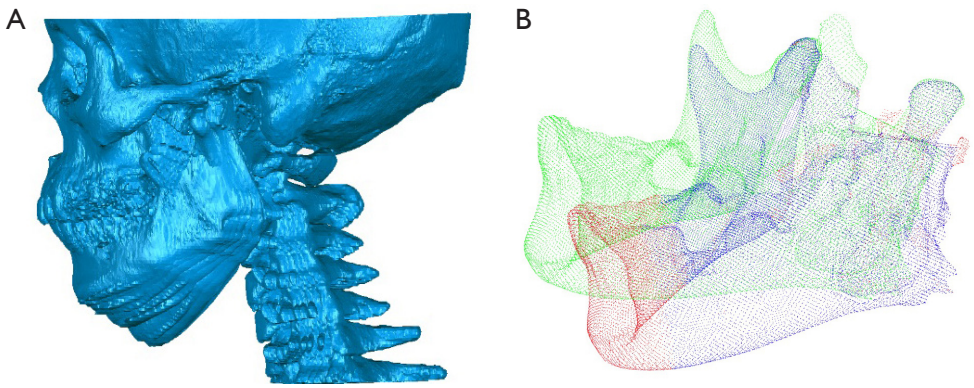

Figure 4 Registration and model of the mandibular movement. (A) 3D model of mandibular mouth-opening movement after registration of maxillary; (B) Mandibular registration point cloud, source point cloud green at the intercuspal position registered to the target point cloud red. After registration, the point cloud is displayed in blue. 3D, 3-dimensional.

Table 1 Information of the normal volunteers

Participant	Gender	Age (years)	MIO (mm)
1	Male	26	42
2	Female	22	38
3	Female	25	39
4	Female	22	41
5	Male	25	43
6	Male	25	42
7	Female	20	39
8	Male	20	41
9	Male	25	40
Average	–	23.8	40.6

MIO, maximum incisor opening.

of the point in the *ith* frame, and R_i and t_i are the rotation matrix and corresponding translation vector of the mandibular movement from the intercuspal position frame to the *ith* frame calculated above, respectively. Then, the trajectories of the highest point of bilateral condyles, the midpoint of mandibular central incisors, were smoothed by the splint function.

The motion curve shape of the highest point of all condyles at the MIO was evaluated. For ease of comparison between normal participants, the curve path of spatial motion from the motion's initial point to the termination point was calculated in the sagittal plane of each point along the condyle, including both prosthetic and natural condyles.

Results

For the normal TMJs, there were 9 volunteers with 18 joints. Of these, 4 were females and 5 were males, with an average age of 23.8 years and an average MIO of 40.6 mm (*Table 1*). The average trajectory for each point was a concave upward curve (*Figure 5*). The arc lengths and average curvature radius were shown in *Table 2*. For P_0, the arc length and curvature radius of the average trajectory were 18.8 and 12.5 mm, respectively. The arc length of the average trajectory decreased from P_0 to P_{-25} and reached 12.2 mm at P_{-25}. The curvature radius of the average trajectory gradually decreased from P_0 to P_{-25} and reached 3.8 mm at P_{-25}. The sum of the Fréchet distance of each point is shown in *Table 3* (*Figure 6*). From P_0 to P_{-20}, the Fréchet distance decreased from 54.88 to 46.78 mm. P_{-20} had the shortest Fréchet distance. The arc length and average curvature radius of its average trajectory were 13.0 and 4.2 mm, respectively.

As for the TMJ TJR, there were 5 patients, including 4 females and 1 male, with an average age of 46.8 years. Among them, 4 had unilateral TJR, and 1 had bilateral TJR. The average postoperative follow-up time was 22 months. The preoperative MIO was 27.8 mm and the postoperative MIO was 40.6 mm (*Table 4*). The trajectories of the contralateral normal joints of patients with unilateral TJR and all condylar prostheses were significantly decreased (*Table 2*). The average arc lengths and curvature radius of P_{-10}, which denoted the corresponding points in the normal joint to the top of the condylar prosthesis, were 15.6/6.6 mm for the normal cases, 13.1/4.9 mm and

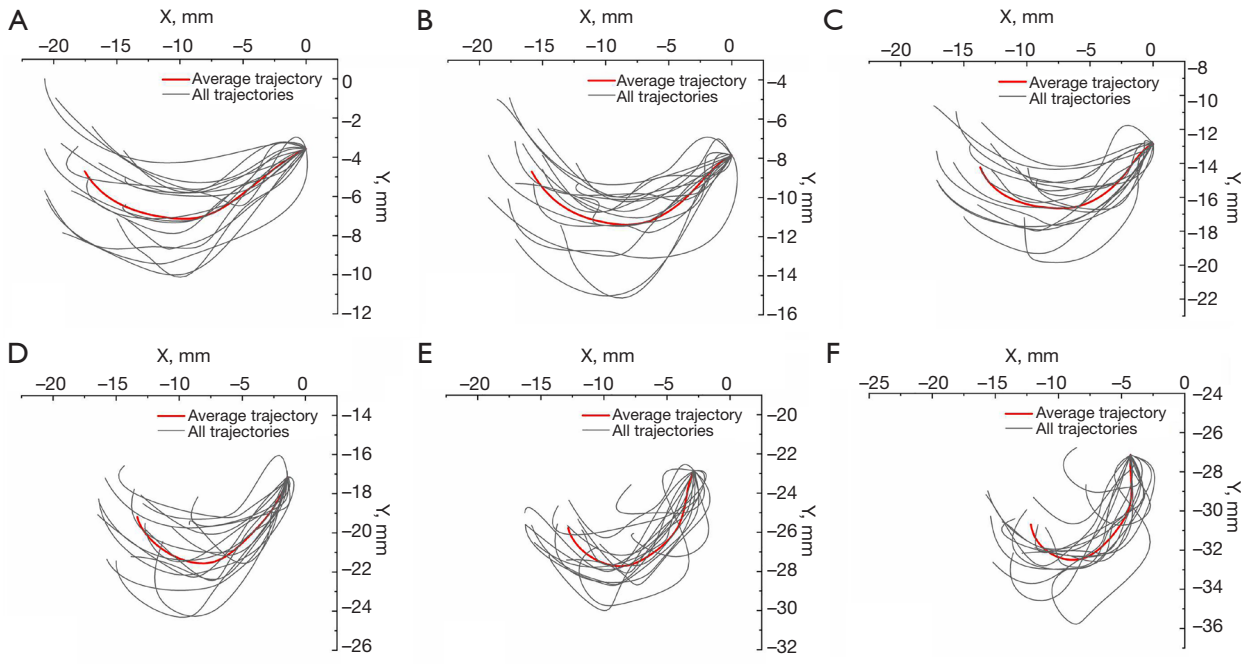

Figure 5 The trajectories of P_0 (A), P_{-5} (B), P_{-10} (C), P_{-15} (D), P_{-20} (E), and P_{-25} (F) moved to the same starting coordinate. The red line represents the average trajectories for each point.

Table 2 Arc length and curvature radius of points in the natural and prosthesis joints

Point (mm)	Natural joints (n=18)		Unilateral TJR (n=4)				Bilateral TJR (n=2)	
	l	r	N l	N r	P l	P r	P l	P r
P_0	18.8	12.5	15.5	4.2	–	–	–	–
P_{-5}	17.4	9.6	14.2	4.5	–	–	–	–
P_{-10}	15.6	6.6	13.1	4.9	4.7	4.4	6.4	5.8
P_{-15}	14.3	5.9	12.1	5.6	3.9	1.1	4.8	4.8
P_{-20}	13.0	4.2	11.3	6.0	3.6	1.2	4.2	1.2
P_{-25}	12.2	3.8	10.7	6.0	4.0	3.1	4.6	1.8
P_{-30}	11.5	3.1	10.2	4.5	5.0	4.5	5.9	4.0
P_{-35}	11.7	2.3	10.0	2.1	6.3	5.5	7.7	4.2
P_{-40}	10.7	2.3	9.9	0.8	7.7	6.4	9.6	5.0
P_{-45}	10.7	2.2	10.1	0.9	9.2	6.8	11.7	4.3
P_{-50}	10.8	2.1	10.8	2.6	10.7	7.1	13.7	3.9
P_{-55}	11.2	2.1	11.4	3.4	12.2	7.5	15.9	3.9

TJR, total joint replacement; N, natural; P, prosthesis; l, arc length; r, curvature radius.

Table 3 Fréchet distance of the 12 point's trajectories

Point	Sum of Fréchet distance (mm)
P_0	54.88
P_{-5}	53.14
P_{-10}	55.46
P_{-15}	48.51
P_{-20}	46.78
P_{-25}	51.84
P_{-30}	51.98
P_{-35}	59.33
P_{-40}	59.16
P_{-45}	63.73
P_{-50}	69.68
P_{-55}	76.61

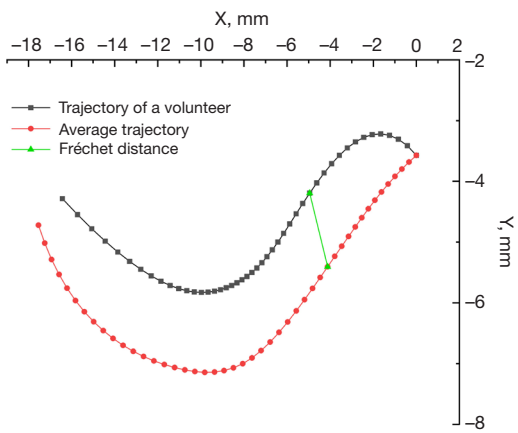

Figure 6 Calculation of the Fréchet distance. The red curve represents the average trajectory of P_0. The black curve represents one trajectory of P_0. The red lines represent the Fréchet distance between the two curves.

4.7/4.4 mm in normal and prosthetic TMJ, respectively, for the unilateral replacement patients, and 6.4/5.8 mm for the bilateral replacement patient, respectively (*Figure* 7). The average trajectories from P_0 to P_{-25} in the normal TMJ and P_{-10} to P_{-25} in the prosthetic TMJ of patients who received TJR are shown in *Figure 8*.

Discussion

Although there are many different methods to analyze condylar motion, such as using an Arcus Digma ultrasound device (12) or a tracking camera system with CT (10,13), dynamic stereometry combining MRI (14), patients are still required to wear tracking devices attached to the teeth or face, which may complicate the measuring procedure and affect the mandibular movement. Jeon *et al.* (26) used a digital camera to record the mouth-opening movement but it failed to show the movement of the condyle. In this study, we used dynamic MRI and CT to study the motion of normal and TJR joints. By using the FIESTA sequence, the scanning time was reduced, and no attached device was needed for patients during the natural mouth-opening process. The FIESTA sequence can generate T2/T1 contrast and offer a good tissue contrast between the joint liquid and the articular disc with a short TR and TE. Although it cannot be 3D-reconstructed and loses motion information in the other planes, it can provide clear anatomic landmarks of the condyle in the sagittal plane (20). Considering the possible influence of the titanium alloy and cobalt-chromium alloy on MRI, we used dynamic CT to study the postoperative motion of the contralateral normal joints and TJR joints in this study. During the scanning, the patient does not need to wear any external devices on their teeth or skin, reducing the time to manufacture personalized devices, and it is especially suitable for patients with dentition defects and dentition loss.

In the present study, we evaluated the motion of normal TMJ and TMJ after alloplastic joint replacement. We chose volunteers aged >18 years for dynamic MRI examination because the TJR patients were >18 years. Additionally, we included TJR follow-up of >6 months with an MIO >30 mm because the patients' mouth opening recovered stable and the motion of the prosthesis will not change after operative trauma; 30 mm was the least recovered MIO relative to normal volunteers. Similar to previous findings (8), the arc length of the average trajectory of the top of the condyle in normal participants was 18.8 mm. The arc length of the average trajectory of the top of the condyle was 5.27 mm in the patient group, which exceeded that reported in previous research (2 mm) (8). This may be due to the smaller sample size in this study or the sliding distance rather than the arc length calculated by Merlini *et al.*

We found the maximum mouth opening improved significantly after alloplastic joint replacement, whereas laterotrusion was restricted. This once again showed that TMJ TJR could substantially improve the quality of life of patients after surgery, as has been established by a large number of previous studies (5-7). A common belief is that

Table 4 TMJ TJR patients

Subject	Gender	Age (years)	Preoperative diagnosis	TJR	Size of the fossa component	Size of the mandibular component (mm)	Follow-up (months)	MIO (mm), pre-/post-op
1	Female	66	OA	Biomet (left)	Small	55	40	18/38
2	Female	48	OA	Biomet (right)	Small	50	12	43/46
3	Male	49	OA	Biomet (right)	Small	45	34	32/34
4	Female	42	OA	Biomet (right)	Small	50	12	18/46
5	Female	29	OA	Biomet (bilateral)	Small	45	12	28/39
Average	–	46.8	–	–	–	–	22	27.8/40.6

TMJ, temporomandibular joint; TJR, total joint replacement; OA, osteoarthritis; pre-/post-op, pre-operation/post-operation; MIO, maximum incisor opening.

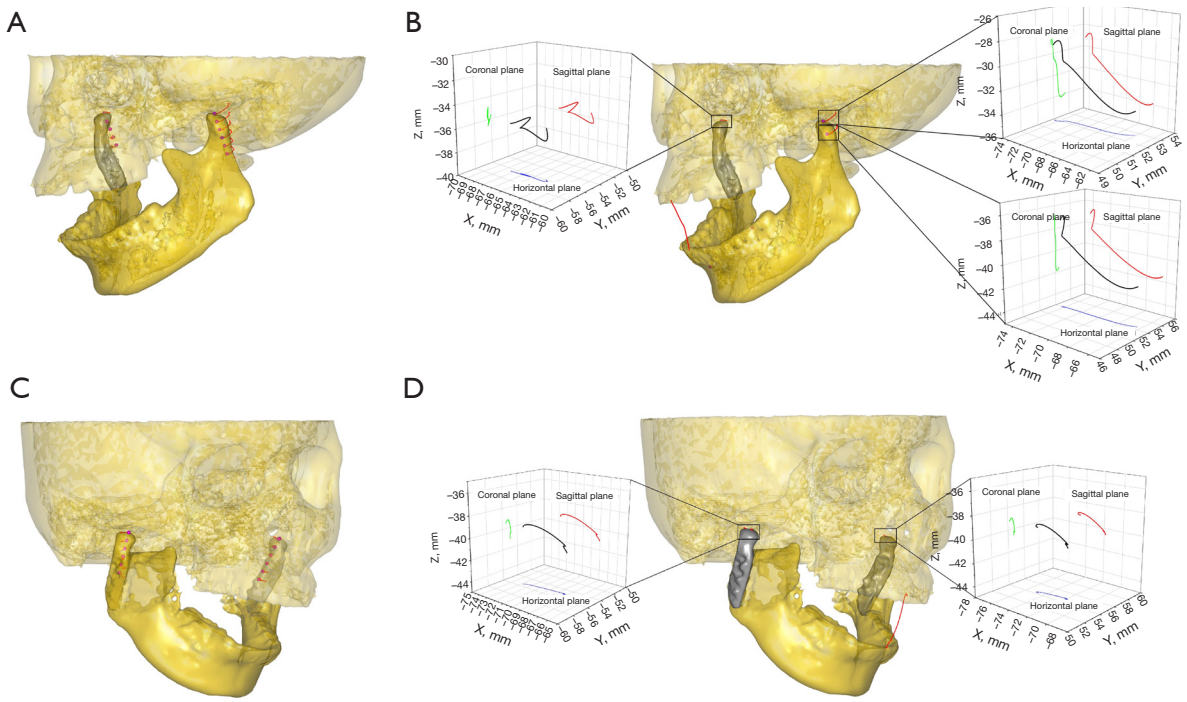

Figure 7 The trajectories from P_0 to P_{-25} in the normal TMJ and P_0 to P_{-25} in prosthetic TMJ (A), and detailed displayed trajectories of the P_{-10} of prosthetic side and the P_0 and P_{-10} in the contralateral normal joint (B) of unilateral replacement patient. Trajectories from prosthetic P_0 to P_{-25} (C), and detailed displayed trajectories of prosthetic P_{-10} of bilateral replacement patient (D). TMJ, temporomandibular joint.

the loss of the external (lateral) pterygoid muscle attachment is an essential factor restricting the sliding of the condylar prosthesis (5,9,10). However, Celebi *et al.* (9) found that the TMJ fossa prosthesis restricted the artificial condyle movement even if the LPM was attached to a cadaver head during the mouth-opening process. Therefore, to restore the mandibular lateral and protrusive movement, it is not only necessary to reattach the LPM, but also to modify the interface between the glenoid fossa and condylar prostheses.

Van Loon *et al.* (10) confirmed the rationality of reducing the compensatory motion on the healthy side by lowering the rotational center of the condylar prosthesis. They pointed out that lowering the rotational center of the condylar prosthesis by 15 mm could minimize the

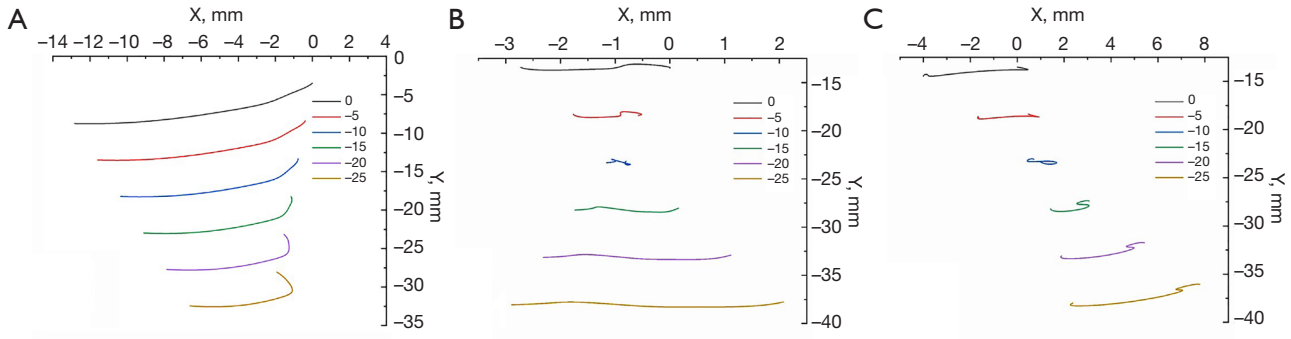

Figure 8 The average trajectories from P_0 to P_{-25} in the normal TMJ (A), P_0 to P_{-25} in the prosthetic TMJ (B) of unilateral replacement patients and the average trajectories from P_0 to P_{-25} in the prosthetic TMJ of a bilateral replacement patient (C). TMJ, temporomandibular joint.

compensatory motion of the healthy side. This concept has been widely adopted in today's prostheses. However, there is no consensus on the optimal descent distance of the condylar prosthesis. Further optimization of the prosthesis design relies on determining the movement from the condyle to the mandibular angle, but there are currently no reports on this. The average arc lengths and curvature radius of normal joints between the condylar head and P_{-20} can provide a reference for prosthesis design, which has also not yet been reported. In the study, we analyzed the trajectory from the top of the condyle to the angle along the ramus during mouth opening. We used the Fréchet distance to determine the point with the most negligible influence of receptor difference. The arc length and curvature radius of the average trajectories gradually decreased from the top to the angle. The point with the most similar trajectories was located 20 mm below the top of the condyle. The arc length and curvature radius of the average trajectory was 13.0 and 4.2 mm, respectively. Our results showed that from P_{-20} to P_0, the similarity of the trajectories decreased. This was probably because as the point got closer to the top of the condyle, the trajectories were influenced by the anatomical form of the glenoid fossa. The location with a low similarity of trajectories was not suitable for the design of standard prostheses. By comparing the trajectories of the corresponding point P_{-10} in the normal TMJ and the top of the condylar prosthesis, we found that the latter was reduced. This is because the LPM was stripped and the loss of function in the TJR joints. The contralateral normal joint's movement was also affected after unilateral TJR implantation.

The range of mandibular motion is different between cases of TMJ TJR among tumor or ankylosis (fibrous or bony) and osteoarthritis patients. In this study, we chose osteoarthritis TJR patients for trajectory analysis because they are close to normal anatomy. Although the sample size was small, including only 4 unilateral TJR patients and one bilateral TJR patient, we developed 2 new methods to measure mandibular joint motion by dynamic MRI and CT, respectively. In the future, various pathological conditions before TJR surgery, as well as increasing the number of TJR cases, are needed using the established method from this study for more comprehensive analysis.

Alloplastic TJR has been shown to be clinically effective in numerous studies. However, the movement of the condyle changes from both sliding and rotation to almost only rotation movement after TJR. This is because the LPM loses its attachment after the operation, resulting in limited mandibular movement (27). It has been suggested that changes in prosthesis design may have improved postoperative jaw kinematics, especially reattaching the LPM's inferior head (LPM-IH) to the prosthetic TMJ to support normal functional occlusion and mandibular motion (28). Mommaerts (29) designed a new prosthesis with a lattice scaffold located in the condylar neck of titanium for the LPM to reattach. However, this prosthesis is prone to a degree of wear in practical application (30), which is due to improved mandibular movement. Thus, the contact surface of the fossa needs to be modified according to normal joint movement. In this study, the trajectory of the joint during opening and closing mouth movements between normal individuals and TJR patients were compared using dynamic imaging methods, which could directly capture the mandibular movement. Since

this is a preliminary study aimed at developing a new approach to measure mandibular joint motion, we only included 5 patients who agreed to undergo a dynamic CT examination in 2020. We believe by our new method of measuring mandibular joint movement for more cases, the modification of TJR prosthesis will be proposed in the future.

Conclusions

In this study, we developed 2 new methods to measure mandibular joint motion. In addition, we found that P_{-20} in the normal joint has the most similar trajectory among individuals. The trajectory difference between the prosthesis apex without LPM attachment and the corresponding point at the normal joint with LPM attachment provides a reference for fossa prosthesis functional surface design.

Acknowledgments

We thank Dr. Edward Ellis 3rd (Department of Oral and Maxillofacial Surgery, University of Texas Health Science Center at San Antonio, TX, USA) for his help with revising the manuscript.
Funding: This study was supported by grants from the Clinical plus project of Shanghai 9th People's Hospital (No. JYLJ201805), the Science and Technology Commission of Shanghai Municipality Science Research Project (Nos. 20Y11903900, and 20S31902500), and the 16th College Student Innovation and Entrepreneurship Training Program of Shanghai Jiao Tong University School of Medicine (No. 1622Y527).

Footnote

Conflicts of Interest: All authors have completed the ICMJE uniform disclosure form (available at https://qims.amegroups.com/article/view/10.21037/qims-22-1239/coif). The authors have no conflicts of interest to declare.

Ethical Statement: The authors are accountable for all aspects of the work in ensuring that questions related to the accuracy or integrity of any part of the work are appropriately investigated and resolved. The study was conducted in accordance with the Declaration of Helsinki (as revised in 2013) and was approved by the Independent Ethics Committee of Shanghai Jiao Tong University School of Medicine Affiliated 9th People's Hospital (No. SH9H-2021-T111-2). Informed consent was provided by all individual participants.

References

1. Mercuri LG, Edibam NR, Giobbie-Hurder A. Fourteen-year follow-up of a patient-fitted total temporomandibular joint reconstruction system. J Oral Maxillofac Surg 2007;65:1140-8.
2. Chen X, Wang Y, Mao Y, Zhou Z, Zheng J, Zhen J, Qiu Y, Zhang S, Qin H, Yang C. Biomechanical evaluation of Chinese customized three-dimensionally printed total temporomandibular joint prostheses: A finite element analysis. J Craniomaxillofac Surg 2018;46:1561-8.
3. Zhao J, Zou L, He D, Ellis E 3rd. Comparison of bone adaptation after modification in biomet standard alloplastic temporomandibular joint prostheses. J Craniomaxillofac Surg 2018;46:1707-11.
4. Leandro LF, Ono HY, Loureiro CC, Marinho K, Guevara HA. A ten-year experience and follow-up of three hundred patients fitted with the Biomet/Lorenz Microfixation TMJ replacement system. Int J Oral Maxillofac Surg 2013;42:1007-13.
5. Mercuri LG, Wolford LM, Sanders B, White RD, Giobbie-Hurder A. Long-term follow-up of the CAD/CAM patient fitted total temporomandibular joint reconstruction system. J Oral Maxillofac Surg 2002;60:1440-8.
6. Wojczyńska A, Leiggener CS, Bredell M, Ettlin DA, Erni S, Gallo LM, Colombo V. Alloplastic total temporomandibular joint replacements: do they perform like natural joints? Prospective cohort study with a historical control. Int J Oral Maxillofac Surg 2016;45:1213-21.
7. Mercuri LG, Wolford LM, Sanders B, White RD,

Hurder A, Henderson W. Custom CAD/CAM total temporomandibular joint reconstruction system: preliminary multicenter report. J Oral Maxillofac Surg 1995;53:106-15; discussion 115-6.
8. Merlini L, Palla S. The relationship between condylar rotation and anterior translation in healthy and clicking temporomandibular joints. Schweiz Monatsschr Zahnmed 1988;98:1191-9.
9. Celebi N, Rohner EC, Gateno J, Noble PC, Ismaily SK, Teichgraeber JF, Xia JJ. Development of a mandibular motion simulator for total joint replacement. J Oral Maxillofac Surg 2011;69:66-79.
10. van Loon JP, Falkenström CH, de Bont LG, Verkerke GJ, Stegenga B. The theoretical optimal center of rotation for a temporomandibular joint prosthesis: a three-dimensional kinematic study. J Dent Res 1999;78:43-8.
11. Kwon JH, Im S, Chang M, Kim JE, Shim JS. A digital approach to dynamic jaw tracking using a target tracking system and a structured-light three-dimensional scanner. J Prosthodont Res 2019;63:115-9.
12. Sójka A, Huber J, Kaczmarek E, Hędzelek W. Evaluation of Mandibular Movement Functions Using Instrumental Ultrasound System. J Prosthodont 2017;26:123-8.
13. Chang AR, Han JJ, Kim DS, Yi WJ, Hwang SJ. Evaluation of intra-articular distance narrowing during temporomandibular joint movement in patients with facial asymmetry using 3-dimensional computed tomography image and tracking camera system. J Craniomaxillofac Surg 2015;43:342-8.
14. Chen CC, Lin CC, Chen YJ, Hong SW, Lu TW. A method for measuring three-dimensional mandibular kinematics in vivo using single-plane fluoroscopy. Dentomaxillofac Radiol 2013;42:95958184.
15. Ettlin DA, Mang H, Colombo V, Palla S, Gallo LM. Stereometric assessment of TMJ space variation by occlusal splints. J Dent Res 2008;87:877-81.
16. Peck CC, Murray GM, Johnson CW, Klineberg IJ. The variability of condylar point pathways in open-close jaw movements. J Prosthet Dent 1997;77:394-404.
17. Abolmaali ND, Schmitt J, Schwarz W, Toll DE, Hinterwimmer S, Vogl TJ. Visualization of the articular disk of the temporomandibular joint in near-real-time MRI: feasibility study. Eur Radiol 2004;14:1889-94.
18. Conway WF, Hayes CW, Campbell RL. Dynamic magnetic resonance imaging of the temporomandibular joint using FLASH sequences. J Oral Maxillofac Surg 1988;46:930-8.
19. Burnett KR, Davis CL, Read J. Dynamic display of the temporomandibular joint meniscus by using "fast-scan" MR imaging. AJR Am J Roentgenol 1987;149:959-62.
20. Sun Q, Dong MJ, Tao XF, Yu Q, Li KC, Yang C. Dynamic MR imaging of temporomandibular joint: an initial assessment with fast imaging employing steady-state acquisition sequence. Magn Reson Imaging 2015;33:270-5.
21. Zou L, Zhong Y, Xiong Y, He D, Li X, Lu C, Zhu H. A Novel Design of Temporomandibular Joint Prosthesis for Lateral Pterygoid Muscle Attachment: A Preliminary Study. Front Bioeng Biotechnol 2021;8:630983.
22. Hu YK, Yang C, Xie QY. Changes in disc status in the reducing and nonreducing anterior disc displacement of temporomandibular joint: a longitudinal retrospective study. Sci Rep 2016;6:34253.
23. Pelliccia L, Lorenz M, Heyde CE, Kaluschke M, Klimant P, Knopp S, Schleifenbaum S, Rotsch C, Weller R, Werner M, Zachmann G, Zajonz D, Hammer N. A cadaver-based biomechanical model of acetabulum reaming for surgical virtual reality training simulators. Sci Rep 2020;10:14545.
24. Erdogan K. Spline interpolation techniques. Journal of Technical Science and Technologies 2013:47-52.
25. Fréchet MM. Sur quelques points du calcul fonctionnel. Rendiconti del Circolo Matematico di Palermo (1884-1940) 1906;22:1-72.
26. Jeon KJ, Kim YH, Ha EG, Choi HS, Ahn HJ, Lee JR, Hwang D, Han SS. Quantitative analysis of the mouth opening movement of temporomandibular joint disorder patients according to disc position using computer vision: a pilot study. Quant Imaging Med Surg 2022;12:1909-18.
27. Wojczyńska A, Gallo LM, Bredell M, Leiggener CS. Alterations of mandibular movement patterns after total joint replacement: a case series of long-term outcomes in patients with total alloplastic temporomandibular joint reconstructions. Int J Oral Maxillofac Surg 2019;48:225-32.
28. Zebovitz E. Total Temporomandibular Joint Prosthetic Reconstruction: The Importance of Lateral Pterygoid Muscle Reattachment to Lateral Excursive and Protrusive Mandibular Movement. J Oral Maxillofac Surg 2021;79:1191-1194.e1.
29. Mommaerts MY. On the reinsertion of the lateral pterygoid tendon in total temporomandibular joint replacement surgery. J Craniomaxillofac Surg

2019;47:1913-7.
30. De Meurechy N, Aktan MK, Boeckmans B, Huys S, Verwilghen DR, Braem A, Mommaerts MY. Surface wear in a custom manufactured temporomandibular joint prosthesis. J Biomed Mater Res B Appl Biomater 2022;110:1425-38.

Cite this article as: Wang J, Hua J, Ding R, Zou L, Li H, Zhang L, Sun Q, He D. Comparative study of normal condyle and temporomandibular joint prosthesis movement during mouth opening by dynamic magnetic resonance imaging and computed tomography. Quant Imaging Med Surg 2023;13(7):4147-4159. doi: 10.21037/qims-22-1239

